Published online before print October 18, 2011
The British Institute of Radiology, doi: 10.1259/bjr/24514638
The British Journal of Radiology

The effect of 6 and 15 MV on intensity-modulated radiation therapy prostate cancer treatment: plan evaluation, tumour control probability and normal tissue complication probability analysis, and the theoretical risk of secondary induced malignancies

[1]M HUSSEIN, MSc, [1]S ALDRIDGE, MSc, [2]T GUERRERO URBANO, PhD, FRCR and [1]A NISBET, PhD

[1]*Department of Medical Physics and* [2]*Department of Oncology, St Luke's Cancer Centre, Royal Surrey County Hospital NHS Foundation Trust, Guildford, Surrey, UK*

Objective: To investigate the effect of 6 and 15 MV photon energies on intensity-modulated radiation therapy (IMRT) prostate cancer treatment plan outcome and to compare the theoretical risks of secondary induced malignancies.
Methods: Separate prostate cancer IMRT plans were prepared for 6 and 15 MV beams. Organ equivalent doses were obtained through thermoluminescent dosimeter (TLD) measurements in a Rando phantom. The neutron dose contribution at 15 MV was measured using polyallyl-diglycol-carbonate (PADC) neutron track etch detectors. Risk coefficients from ICRP Report 103 were used to compare the risk of fatal secondary induced malignancies in out-of-field organs and tissues for 6 and 15 MV. For the bladder and the rectum, a comparative evaluation of the risk using three separate models was carried out. Dose–volume parameters for the rectum, bladder and prostate planning–target–volume were evaluated, as well as normal tissue complication probability (NTCP) and tumour control probability (TCP) calculations.
Results: There is a small increased theoretical risk of developing a fatal cancer from 6 MV compared with 15 MV, taking into account all the organs. Dose–volume parameters for the rectum and bladder show that 15 MV results in better volume sparing in the regions below 70 Gy, but the volume exposed increases slightly beyond this in comparison to 6 MV, resulting in a higher NTCP for the rectum of 3.6% versus 3.0% ($p=0.166$).
Conclusion: The choice to treat using IMRT at 15 MV should not be excluded, but should be based on risk versus benefit, considering the age and life expectancy of the patient together with the relative risk of radiation-induced cancer and NTCPs.

Received 4 November 2010
Revised 26 January 2011
Accepted 1 February 2011

DOI: 10.1259/bjr/24514638

Three-dimensional conformal radiation therapy (3D-CRT) is most commonly delivered with high-energy photons, typically in the range of 6–18 MV. Intensity-modulated radiation therapy (IMRT) is known to improve target coverage and provide better organ at risk (OAR) sparing in comparison with 3D-CRT [1]. However, IMRT is associated with an increase in the number of monitor units (MU) relative to 3D-CRT, which has led to concerns about a potential increased risk of radiation-induced malignancies [2]. This risk becomes more relevant at higher photon energies (>10 MV), where there is a possibility of greater leakage radiation, treatment head scatter, patient scatter and photo-neutron contribution [3]. Subsequently, the majority of IMRT treatments being delivered in the UK today are with 6 MV photons. The use of higher energies for deep-seated tumours, such as in the prostate, have been favoured by some as providing better dose coverage to the tumour target, while also improving normal tissue sparing [4].

Address correspondence to: Mr Mohammad Hussein, Department of Medical Physics, Royal Surrey County Hospital, Egerton Road, Guildford, Surrey, GU2 7XX, UK. E-mail: m.hussein@nhs.net

It has been reported in the literature that IMRT may double the risk of fatal second cancers compared with 3D-CRT [5–9]. The risk of fatal cancer has been reported for 6 MV 3D-CRT and IMRT prostate treatments to vary by 0.6–1.5% and 1–3.0%, respectively [7, 8, 10]. For 15 MV photons, the risk has been reported to be 3.4% [10]. These values have been computed using data from the National Council on Radiation Protection and Measurements (NCRP) Report 116, assuming a linear lifetime risk value of 0.05 per Sv for all fatal radiation-induced cancers for the general population [11].

There is as yet no epidemiological data for radiation-induced malignancy in patients with prostate cancer who received treatment with IMRT. A modest increase in second malignancies of 1 in 70 patients undergoing radiation and surviving more than 10 years was reported for 3D-CRT, with most common sites for secondary cancers being the bladder and rectum [12].

Currently, at our centre (St Luke's Cancer Centre, SLCC), 3D-CRT to the prostate is delivered mostly with 15 MV photons, whereas IMRT is delivered with 6 MV photons. During the initial set-up of prostate IMRT at SLCC, all energy beams (6, 10 and 15 MV) were in

clinical use. After 10 patients had been treated it was decided by the clinical team to use only 6 MV photons until the use of higher energy beams was further evaluated, given that the potential advantages related to their use could be offset by a potential increase in the risk of second malignancy.

This study has investigated whether high-energy IMRT offers better target coverage and normal tissue sparing for prostate cancer. This work has investigated the organ equivalent doses through thermoluminescent dosimeter (TLD) measurement in an anthropomorphic Alderson radiation therapy human phantom (''Rando'') in order to assess the theoretical risk of secondary malignancies in organs and tissues distant from the tumour target. For the bladder and rectum, a comparative evaluation of calculating the risk using the linear non-threshold model [13–15], linear-plateau model [16] and initiation-inactivation model [17] was performed. The neutron dose contribution at 15 MV was estimated using polyallyl-diglycol-carbonate (PADC) neutron track etch detectors. Dosimetric plan evaluations were carried out for the planning target volume (PTV) and OARs, as well as an assessment of the total number of MU for plans generated with different energies.

Methods and materials

Treatment planning

The planning scans of five patients who had completed a course of radical radiotherapy to the prostate were used. Patients were scanned according to departmental protocol using 2.5 mm slices from the sacro-iliac joints to the penile urethra. All patient details were anonymised. Prostate volumes were not outlined by the same oncologist. Outlining was carried out by the clinician treating each patient and was standardised by protocol. Outlining has been tested against protocol in the form of outlining exercises. Organs at risk included the bladder, rectum, femoral heads and bowel. IMRT plans at 6 and 15 MV for the five different planning scans were generated using the inverse-planning Helios optimisation tool in the Varian Eclipse treatment planning system (Varian Medical Systems Inc., Palo Alto, CA) and volume dose calculations were performed using the pencil beam convolution algorithm. Target volume definition, plan objectives and constraints followed the protocol set out in the Conventional or High Dose Hypofractionated IMRT for Prostate Cancer (CHHiP) trial [18]. For this study, the conventional fractionation of 74 Gy in 2 Gy per fraction was used in the IMRT treatment planning and measurements.

The prostate IMRT plans were generated adopting a 5–radiation–beam arrangement incorporating a left and right anterior oblique field (LAO and RAO), a left and right posterior oblique field (LPO and RPO), and a posterior field (POST). The same beam angles were used for 6 and 15 MV plans for each CT dataset. In order to reduce uncertainty in the planning process, all plans were optimised at 6 MV, and subsequently recalculated and optimised at 15 MV using a pre-defined optimisation template as a starting point. All plans were normalised such that the median target dose was 100%.

Assessment of the dose–volume parameters for the prostate PTV, rectum and bladder were analysed for each plan at 6 and 15 MV. For the prostate PTV the parameters that were compared were $D_{99\%}$ (minimum dose delivered to 99% of the volume), $D_{95\%}$, $D_{50\%}$, $D_{5\%}$ and the 95% conformity index ($CI_{95\%}$; *i.e.* the ratio of the irradiated volume receiving 95% of the prescribed dose and the volume of the PTV).

Although dose constraints for the bladder and rectum are usually specified in terms of percentage volume, it was only possible to compare the doses received in terms of absolute volume in cm^3 between different plans due to the variability in the size of these organs between the five cases. Therefore, for the rectum and bladder, the dose parameters investigated were $V30_{Gy}$ (volume receiving 30 Gy), $V40_{Gy}$, $V50_{Gy}$, $V60_{Gy}$, $V70_{Gy}$ and $V74_{Gy}$. In all cases, the dose to the bowel and femoral heads were within CHHiP trial constraints and no further evaluation was performed.

Radiobiological evaluation

To determine whether there is a biological effect due to a potential difference in target volume dose heterogeneity between 6 and 15 MV, tumour control probability (TCP) calculations were performed in BIOPLAN [19] using the mechanistic Poisson-based TCP model [20]. The following input parameters for the TCP models for prostate tumours were used: radiosensitivity parameter $\alpha=0.29\ Gy^{-1}$, interpatient variation in radiosensitivity parameter $\sigma_\alpha=0.07\ Gy^{-1}$, clonogenic cell density $\rho_c=10^7\ cm^{-3}$ and an α/β ratio of 10 [21]. These parameters have been fitted to clinical data from patients with intermediate risk disease. Although it has recently been suggested that an α/β ratio of 1.5 is more appropriate [22], use of this value in conjunction with the fitted parameters resulted in TCP>99%, which means that these parameters put the prescribed dose in the insensitive part of the TCP curve (*i.e.* large changes in dose would be required to affect TCP), which is not consistent with clinical data. Using a value of 10 for α/β gave TCP in the region of 80%. For example, Zelefsky et al [23] reported 8-year actuarial prostate-specific antigen (PSA) relapse-free survival rates of 78% for intermediate-risk patients treated to 81 Gy in 1.8 Gy daily fractions using IMRT (using the Houston definition for biochemical relapse). There are some uncertainties in using TCP models to accurately predict outcome in prostate cancer [24], but for the purpose of our evaluation the parameters mentioned above were deemed suitable for estimating changes in TCP between 6 and 15 MV.

Normal tissue complication probability (NTCP) calculations were performed for the rectum using the Lyman–Kutcher–Burman model [25–27], generalised uniform dose concept [28] and Quantative Analysis of Normal Tissue Effects in the Clinic [29] recommended best parameter estimates of $\alpha/\beta=3$ Gy, volume effects parameter $n=0.09$, slope parameter $m=0.13$, and the dose for 50% complication probability (TD50)=76.9 Gy. For the bladder, there is limited NTCP parameter data due to difficulties in fitting parameters to genitourinary toxicity [30, 31]. The general consensus is to use the Emami–Burman parameters of $n=0.5$, $m=0.11$, and TD50=80 Gy, in conjunction with $\alpha/\beta=3$ Gy [28, 32].

Thermo-luminescent dosimeter measurement

Thermo-luminescent dosimeter (TLD) measurements were performed in an anthropomorphic Alderson radiation therapy (ART) phantom known as Rando, at both 6 and 15 MV for the 5 different treatment plans delivered to the Rando phantom using a Varian Clinac iX (Varian Medical Systems Inc., Palo Alto, CA). The Rando phantom available for this study was version ARTF 1025, which represents a human 1.55 m tall and weighing 50 kg. The phantom is transected horizontally, and each 2.5 cm slice has holes that are plugged with soft tissue equivalent and lung tissue equivalent 5 mm diameter pins that can be replaced by TLD holders [33]. The phantom was CT scanned without TLDs, according to the IMRT protocol at SLCC, using 2.5 mm slices. Once the treatment plan for a particular planning scan was complete, it was possible to copy the plan from a patient onto the Rando phantom image set with the same beam geometry, actual fluences and MUs. It was then possible to deliver a plan on the phantom with TLDs in place.

The TLDs used were the Harshaw TLD-700 lithium fluoride doped with traces of magnesium and titanium (LiF:Ti,Mg) square $3.2 \times 3.2 \times 0.89$ mm chips (Thermo Fisher Scientific Inc., Waltham, MA). The chips were all calibrated separately at 6 and 15 MV against a Farmer-type ionisation chamber, with each single chip given its own sensitivity. Their dose response was determined by irradiating sets of 10 TLDs with doses ranging from 0–400 cGy. The TLDs were read out using a QADOS Harshaw 5500 reader with pre-heat at 145°C for 10 seconds and a temperature ramp of 17°C per second up to a maximum temperature of 300°C for 10 seconds. The TLDs were annealed after each use in a dedicated oven at 400°C for one hour, followed directly by 100°C for 2 hours.

Around 130 TLDs were available for use and these were distributed uniformly throughout the phantom. Where possible, three TLDs were placed at a particular position in order to reduce uncertainties in dose measurement. Skin measurements were performed by placing 20 TLDs on the surface.

The most radiosensitive organs (according to the recommendations in ICRP Report 103 [34]) were outlined on the phantom with reference to bony landmarks. The small and large intestines were not outlined; however, an estimate of the volume was made. One could then estimate the average absorbed dose to each organ based on the TLD positions and measurements, and thus estimate an equivalent dose to each organ.

The red bone marrow, which is important in order to assess the risk of a fatal incidence of leukaemia, was not outlined. In order to be able to estimate the dose to the red bone marrow, the work by Ellis [35] that described the distribution of the active red bone marrow in a normal 40-year-old male was employed. Therefore the average red bone marrow dose, D_{RBM}, was calculated using Equation (1), derived from the data of Ellis:

$$D_{RBM} = 0.13D_{Brain} + 0.08D_{Thyroid} + 0.11D_{Heart} + 0.03D_{C-Spine} + 0.14D_{T-Spine} + 0.11D_{L-Spine} + 0.14D_{Sacrum} + 0.26D_{FH}, \quad (1)$$

where D_{Brain} is average dose to the brain, $D_{Thyroid}$ is the average dose to the thyroid, D_{Heart} is the average dose to the heart, $D_{C\text{-}spine}$ is the average dose to the cervical spine, $D_{T\text{-}Spine}$ is the average dose to the thoracic spine, $D_{L\text{-}Spine}$ is the average dose to the lumbar spine, D_{Sacrum} is the average dose to the sacrum, and $D_{F–H}$ is the average dose to the femoral heads.

Polyallyl-diglycol-carbonate detector neutron track etch detector measurement

Polyallyl-diglycol-carbonate detectors (PADC) were provided and processed by the Computational Dosimetry Group from the Radiation Protection Division of the Health Protection Agency (HPA-RPD; formerly the National Radiological Protection Board). The PADCs themselves were encased in a plastic holder, which induces secondary protons from the neutron interaction. The ionisation caused by the protons in PADC dosimeters forms small weaknesses in its polymeric structure. These weaknesses become vulnerable to attack by an etchant (in this case sodium hydroxide). This may then be blown up into a larger hole using electrochemical etching. In this procedure, the PADC dosimeters were chemically etched for 8 hours and then electrochemically etched for 11½ hours at about 1200 volts. The dosimeters are then scanned and the number of holes present counted by computer software. The PADCs were calibrated at the HPA-RPD using a ^{241}Am-Be source. The PADCs were positioned at 35 cm from the source and exposed for 2 hours, giving them a dose of 2 mSv.

A total of 35 PADC detectors were placed on the surface of the Rando phantom. The phantom was then irradiated three times using the 15 MV IMRT treatment for the plan with the largest irradiated volume. It has been reported that the neutron dose rate at the isocentre is 0.002 Sv (neutron) per Gy (photon), and that the average energy of neutrons produced at the isocentre for 15 MV photons is about 0.4 MeV [36]. The neutron equivalent doses were reported in the operation quantity personal dose equivalent at 10 mm depth in tissue, $H_p(10)$. The response of the PADC was determined by folding the fluence response characteristics of the PADC with the fluence-energy photo-neutron distribution for a linear accelerator using a program developed at HPA-RPD [37]. The folding program uses an algorithm to determine the ratio of the reading of the PADC detector to the true dose equivalent. The photo-neutron energy spectra used in order to fold the response of the PADC detectors were measured by Thomas et al [38]. The average calculated response for the PADCs, after calibration, was determined to be 175 tracks mSv^{-1}.

Out-of-field organ risk of secondary induced cancer estimation

Organ absorbed doses were converted to organ equivalent doses in terms of Sv using the radiation weighting factor [34]; for photons this weighting factor is unity, and therefore the two quantities were equal. The risk of secondary induced malignancy in specific organs was then calculated using risk coefficients taken from ICRP 103 [34], which are given in % Sv^{-1}. The TLD photon data of this study was compared with data by

Howell et al [39] and Kry et al [40], who performed measurements at 6, 15 and 18 MV for dynamic MLC delivery and step-and-shoot IMRT, respectively. The organs compared were the thyroid, stomach, liver and lung. Both studies reported the out-of-field doses in units of μSv MU^{-1}, and therefore the same was done in order to compare the data.

Assessing the risk of secondary cancer in irradiated volume using three different models

Models based on atomic bomb survivors are valid for low doses but cannot be easily related to the higher doses received by OARs [16]. The effect of beam energy on the risk of inducing secondary bladder, rectum or leukaemia was assessed using three different models. The first was to use the linear non-threshold (LNT) model, which assumes a proportional increase of the risk of cancer with radiation dose [13–15]. The second model used was the linear-plateau model, which assumes that the risk saturates at 4 Gy and above [16]. The third model was the non-linear competition model, which takes into account the induction of carcinogenic mutations and cellular survival using Equation (2) and (3).

$$Risk = \frac{\sum_i v_i \times Risk(D_i)}{\sum_i v_i}, \quad (2)$$

where v_i is the volume of tissue receiving dose D_i given in n individual fractions and $Risk(D_i)$ is given by the non-linear dose–response relationship of the competition model. ICRP 103 risk coefficients were used. Where the effect can be calculated using the modified UNSCEAR equation [17], taking into account fractionation, n,

$$Risk(D_i) = \left(aD_i + \frac{bD_i^2}{n}\right) \exp\left[-\left(\alpha D_i + \frac{\beta D_i^2}{n}\right)\right], \quad (3)$$

where a and b are coefficients for the linear and quadratic terms for stochastic effects respectively, and α and β are the coefficients for the linear and quadratic terms for cell killing, respectively. For each of the three models, differential DVHs for the bladder and rectum were used to calculate the risk in every dose interval of the DVH, and then one integrates over the total intervals to give the result [16]. For leukaemia, equation 1 was used in conjunction with equations 2 and 3 to calculate the theoretical risk, taking into account distribution of red bone marrow in the human body.

Estimating the total lifetime and 40-year post-exposure risk

The probability of any fatal cancer is calculated using the out-of-field and in-field organs using Equation (4):

$$Total\ Risk = R_{Thyroid} \cup R_{Lungs} \cup R_{Oesoph} \cup R_{Stomach} \cup R_{Liver} \cup R_{Colon} \cup R_{Skin} \cup R_{Gonads} \cup R_{Leaukaemia} \cup R_{\mathrm{Rectum}} \cup R_{Bladder} \quad (4)$$

The risk of fatal cancer up to 40 years after exposure and the lifetime risk for different age ranges were calculated using age-dependent risk coefficients from Muirhead et al [41]. The majority of the total risk is estimated by the out-of-field calculated risks. These used population-averaged risk coefficients from ICRP 103 (age range 0–80 years). A median 40 years old at age of exposure was therefore assumed. To this end, the age-dependent risk coefficients given by Muirhead et al were normalised at 40 years old at age of exposure to deduce correction factors for the 40-year and lifetime risk to apply to the calculation in Equation (4).

Statistical and uncertainty analysis

Statistical analysis comparing 6 and 15 MV second cancer risk, TCP and NTCP, and dose volume parameters was carried out using the paired two-sample two-tailed t-test for the means where statistical significance was $p<0.05$. TLD uncertainty was calculated as the standard error of the mean for each set of TLDs placed in a certain location and was also a combination of the uncertainty in the individual chip response (1%) and calibration (3%). The estimated uncertainty in the PADC dose was ±10% and was a combination of the uncertainty in the PADC measurement (±2.5%) as well as the uncertainty in the photo-neutron energy spectra used to fold the response of the PADC (±13%) [38]. It is difficult to predict the accuracy of the risks calculated as the coefficients are based on an entire population. For this reason, the risk factors presented in this study should be regarded as relative rather than absolute.

Results

Prostate PTV volumes varied between 57–148 cm^3, with a standard deviation of 34 cm^3. The dose-volume parameters for the prostate PTV at 6 and 15 MV are summarised for all plans in Table 1. Table 2 shows the dose-volume parameters for the rectum and bladder at both energies. In all plans, no rectal volume received 100% dose. In terms of sparing, it was found for both the rectum and bladder that 15 MV was better at sparing in the lower doses, but at doses above 70 Gy there was a small increase in the volumes irradiated. In all plans the bowel and femoral head tolerances were within the CHHiP constraints [18]. Rectal NTCP was found

Table 1. Average prostate PTV dose parameters for all plans

	Minimum dose delivered (%)				
Volume (%)	6 MV	S.D.	15 MV	S.D.	p-value
99	97.4	0.8	97.9	0.5	0.373
95	98.4	0.4	98.7	0.2	0.423
5	101.3	0.2	101.2	0.3	1.000
$CI_{95\%}$	1.57	0.09	1.65	0.10	0.001
TCP	80.4	1.3	80.1	1.4	0.049

Table 2. Average volume dose parameters for rectum and bladder for all plans

Dose (Gy)	Volume receiving dose (cm^3)									
	Rectum					Bladder				
	6 MV		15 MV			6 MV		15 MV		
	Average	SD	Average	SD	*p*-value	Average	SD	Average	SD	*p*-value
30	45.4	12.7	42.2	12.4	0.063	131.3	25.2	121.4	21.8	0.012
40	33.5	9.2	29.7	8.5	0.011	94.4	15.6	88.3	14.6	0.007
50	23.7	6.3	22.0	6.4	0.060	71.5	9.9	67.8	11.8	0.053
60	15.1	3.7	14.6	4.2	0.519	52.2	7.8	50.8	8.1	0.292
70	3.4	1.5	4.0	1.0	0.662	25.5	7.9	27.8	9.6	0.107
74	-	-	-	-		6.3	3.0	7.2	4.8	0.730

to be 3.0%±0.9% for 6 MV and 3.4%±1.1% for 15 MV (p=0.166). Bladder NTCP was calculated to be 0% for both 6 and 15 MV; however, this is unlikely to be clinically meaningful and is a reflection of the scarcity of data, as well as the difficulties in fitting parameters to genitourinary toxicity.

The average number of MUs delivered per prescribed Gy of photon for the different energies was lower for the 15 MV plans at 294±12 MU Gy^{-1} *vs* 351±17 MU Gy^{-1} for 6 MV.

TLD doses were averaged in each slice and doses were plotted starting at 5 cm from the PTV target. The average TLD doses at 6 and 15 MV averaged over the five patients are shown in Figure 1. The results show an almost exponential decrease in the dose with increased distance from the PTV and towards the head of the phantom.

The neutron equivalent doses recorded ranged between 0.5–3.6 mSv per photon Gy (*i.e.* for a 74 Gy treatment the neutron equivalent dose range was 37–263 mSv). PADC doses have also been plotted on Figure 1, and this shows that the neutron dose drops only slightly with increasing distance from the isocentre. The highest dose was not received by the PADC placed on the central axis, but by those either side. The reason is that the PADCs either side of the central axis were in the most collimated part of the beam, where photoneutron production is expected to be greatest. For the PADC placed in the centre of the irradiated field, the overall dose recorded was equivalent to a dose of 2.0±0.3 mSv per photon Gy, which agrees well with reported neutron dose rates at the isocentre of 0.002 Sv (neutron) per Gy (photon) for 15 MV [36]. The composite of neutron and photon dose appeared to be almost double that of the photon-only dose for the out-of-field organs. The neutron dose measured in the in-field region appeared to be negligible against the higher photon dose (around 0.2% contribution). However, this neutron dose is estimated as an entrance surface dose, and is indeed an overestimate of the dose at depth. More detailed organ dosimetry, using Monte Carlo, is planned using voxel-based anthropomorphic phantoms.

Average organ photon equivalent doses for all five patients are summarised in Figure 2, per Gy photon. The organs to receive the highest out-of-field doses were the gonads and colon. In all cases, the doses due to 15 MV photons were lower than for 6 MV. Photon organ equivalent doses per MU in the current study agree reasonably well with published data for both energies (Table 3).

The estimated secondary induced cancer risk for out-of field organs is shown in Table 4. Table 5 shows the

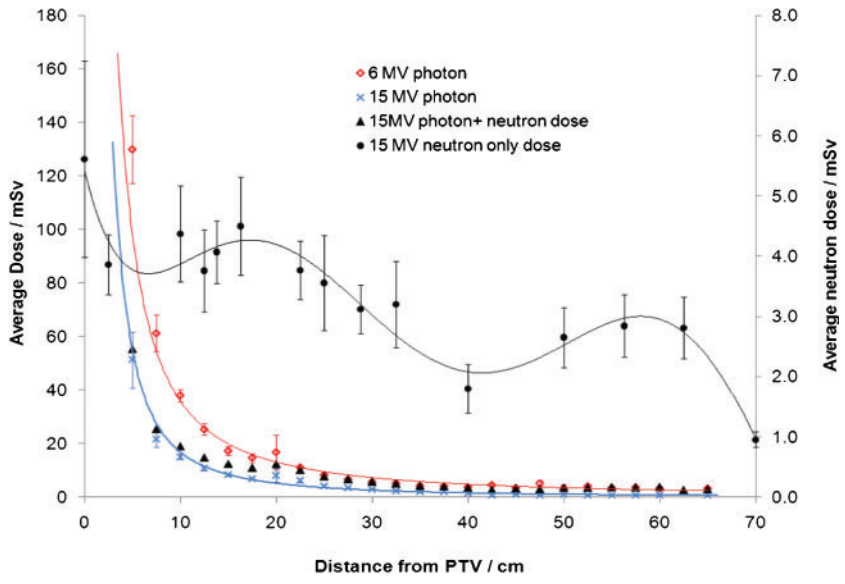

Figure 1. Average TLD doses in each phantom slice as a function of distance away from the isocentre.

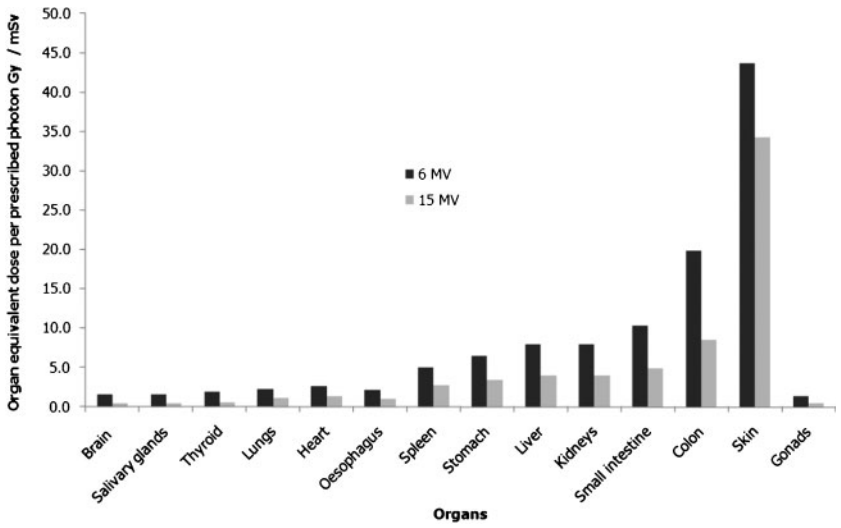

Figure 2. Average photon organ equivalent doses per prescribed photon Gy given for various out-of-field organs.

calculated risk of developing a fatal secondary cancer for the bladder and rectum using the three different risk models.

The probability of any secondary cancer calculated using Equation (4) was found to be 2.8% for 6 MV and 1.6% for 15 MV ($p<0.001$). Age-corrected calculations are shown in Figure 3 for the 40-year risk and Figure 4 for the lifetime risk of fatal cancer. Using the combined photon and neutron dose at 15 MV for the single measurement, it was found that the calculated total risk was 1.3 times that of the photon-only risk (*i.e.* if this factor is applied to all patients then the average total risk at 15 MV would become around 2.0%).

The results show an increased risk of developing a fatal cancer from 6 MV compared with 15 MV. As one would expect, the peak age range where the risk is highest is 40–59 years old, the lowest age range considered in this study. The risk decreases above 70 years old and significantly above 80 years. This is mainly due to different life expectancy.

Discussion

Several authors have investigated the out-of-field doses to organs distant from the tumour volume. Most studies have concentrated on prostate cancer, as this is the most common site for IMRT, as well as having a good treatment prognosis. Thermoluminescent dosimeter (TLD) measurements have been performed by various investigators at IMRT energies ranging from 6–18 MV for step-and-shoot IMRT [40] and dynamic multi-leaf collimation (MLC) delivery [36, 42]. Howell et al [39] compared 3D-CRT with IMRT and deduced an effective dose to the out-of-field organs of 0.0543 Sv Gy^{-1} and 0.0554 Sv Gy^{-1} for 6 and 18 MV, respectively. It has been reported that the photon equivalent dose decreases exponentially with distance [40]. Our study is in agreement with these findings. Recently, Ruben et al [43] compared scatter, leakage, relative contributions of internal patient scatter, collimator and head leakage for 6 MV 3D-CRT versus IMRT using a customised water bath. They found that linac scatter and leakage was the dominant source of secondary dose; this was reported to be 65% of the total secondary dose, whereas for 3D-CRT the dominant source was internal patient scatter (70%).

Epidemiological studies investigating the incidence of second cancer following conventional radiotherapy have reported that most secondary sarcomas and a high proportion of carcinomas occur within 5 cm of the field edge [44]. In this study it was found that within this region the 6 MV dose was higher than that at 15 MV. This can be explained by greater scatter at 6 MV than at 15 MV. Further away from the target, the dose is still lower at 15 MV compared to 6 MV. Higher energies result in greater leakage; however, in this case this is balanced by the lower amount of MUs needed in the IMRT plans compared with 6 MV (this being around 16% lower at 15 MV). The combination of lower scatter and lower MU at higher energies would explain the photon dose difference seen in Figure 1.

The neutron equivalent doses measured in our study to be 0.5–3.6 mSv per 15 MV photon Gy compared with Reft et al [45], who calculated neutron equivalent doses

Table 3. Comparison of photon organ equivalent doses per monitor unit of the current data and published data

Organ	Organ equivalent dose in μSv per MU					
	This study		Kry et al [40]		Howell et al [39]	
	6 MV	15 MV	6 MV	15 MV	6 MV	15 MV
Thyroid	2.7	1.0	2.6	1.8	2.3	1.7
Stomach	9.1	5.7	8.2	8.0	3.3	3.1
Lung	3.2	1.9	3.7	3.8	2.4	2.0
Liver	11.2	6.7	8.2	7.9	3.7	3.7

Table 4. Calculated risk of developing a lifetime fatal secondary malignancy by organ site, given both as a percentage and a fraction

Organ	6 MV			15 MV (photon)				15 MV (corrected for neutron dose)
	Calculated risk (%)	SD	Risk of 1 in	Calculated risk (%)	SD	Risk of 1 in	*p*-value	Calculated risk (%)
Thyroid	0.01	0.002	10134	0.003	0.0003	34393	0.020	0.01
Lungs	0.14	0.019	701	0.07	0.01	1422	0.029	0.13
Oesophagus	0.05	0.008	2049	0.02	0.004	4305	0.035	0.06
Stomach	0.53	0.071	188	0.27	0.04	365	0.076	0.40
Liver	0.09	0.009	1131	0.04	0.01	2296	0.039	0.06
Colon	1.25	0.097	80	0.54	0.06	187	0.006	0.63
Skin	0.004	0.003	24651	0.003	0.01	36862	<0.001	0.10
Gonads	0.08	0.004	1253	0.03	0.003	3546	0.001	0.10
Leukaemia	0.25	0.06	394	0.18	0.10	566	0.151	0.18

at 18 MV using Cr-39 track etch detectors at 2–6 mSv per photon Gy. In our study, the neutron equivalent doses translated to an effective dose of 1 mSv, which contributed to 2% of the photon effective dose at 15 MV. Other studies have reported a neutron dose equivalent of 33 mSv in the target volume and OARs at 15 MV for a dose delivery of 81 Gy [46], and that neutron equivalent doses were independent of distance, decreased with increasing depth in a patient and were a significant contributor to out-of-field doses [47]. Furthermore, Kry et al [47] have carried out Monte Carlo calculations for out-of-field photon and neutron dose in a Rando phantom for 6 and 18 MV photons, and have reported that there was a small difference in the risk of secondary cancer between the two energies.

We found that for all out-of-field organs there was at least a doubling of the risk of developing a fatal cancer due to photons only at 6 MV relative to 15 MV ($p<0.05$ for all organs, except for the stomach, where $p=0.076$). There was a moderate increased risk at 6 MV for leukaemia ($p=0.151$). After correcting for neutron dose, it was found that the risks were comparable. For rectum and bladder risk, the DNA competition model shows a slightly higher risk at 15 MV ($p=0.018$), which may be attributed to the better sparing of IMRT (*i.e.* a larger volume of the rectum or bladder receiving lower doses). Comparison between the risk using the DNA competition, linear-plateau and LNT models shows that the LNT model would provide unrealistic risk estimates for these organs. The estimates provided by the linear-plateau model are more consistent with clinical evidence. A modest increase in second malignancies of 1 in 70 patients undergoing radiation and surviving more than 10 years has previously been reported for 3D-CRT, with most common sites for secondary cancers being the bladder and rectum [12].

An interesting finding was the slightly raised rectal NTCP at 15 MV compared with 6 MV (3.6% compared with 3.0%, respectively). This is due to the fact that, while 15 MV performs better at sparing the rectum at doses below 70 Gy, an extra volume of around 1 cc received doses above 70 Gy compared to 6 MV. Also, if the competition model is true, then the risk of secondary rectal cancer is also slightly increased at 15 MV because a greater volume received less than 30 Gy. It was also observed that the $CI_{95\%}$ was slightly better at 6 MV, indicating better target homogeneity. There also appears to be a reduction in TCP of around 0.3% at 15 MV compared with 6 MV ($p=0.049$); however, it is unlikely that this would have clinical significance.

It has been noted by Sachs and Brenner [48] that the competition model may underestimate the risk at high doses, and those authors have reported a biologically based and minimally parameterised model that incorporates carcinogenic effects, cell killing and proliferation/repopulation effects that were consistent with clinical data for high-dose second cancer incidence in Hodgkin's lymphoma and breast cancer patients. This model was later extended by Shuryak et al [49] for radiation-induced leukaemia to include long-range migration through the bloodstream of haematopoietic stem cells from distant locations. Future evaluations of the risks using these models are planned.

There are other limitations to this method of experimentally deducing cancer risk. Different patients have different anatomy, and it is difficult to make an accurate assessment of different organ risks specific to an individual patient. However, it should be noted that

Table 5. Calculated risk of developing a lifetime fatal secondary malignancy for the rectum and bladder

Risk model	Bladder			Rectum		
	6 MV	15 MV	*p*-value	6 MV	15 MV	*p*-value
LNT (%)	9.24	8.84	<0.001	20.7	19.9	0.003
LP (%)	0.876	0.860	0.233	2.50	2.49	0.213
Competition (%)	0.15	0.17	0.010	0.14	0.17	0.018

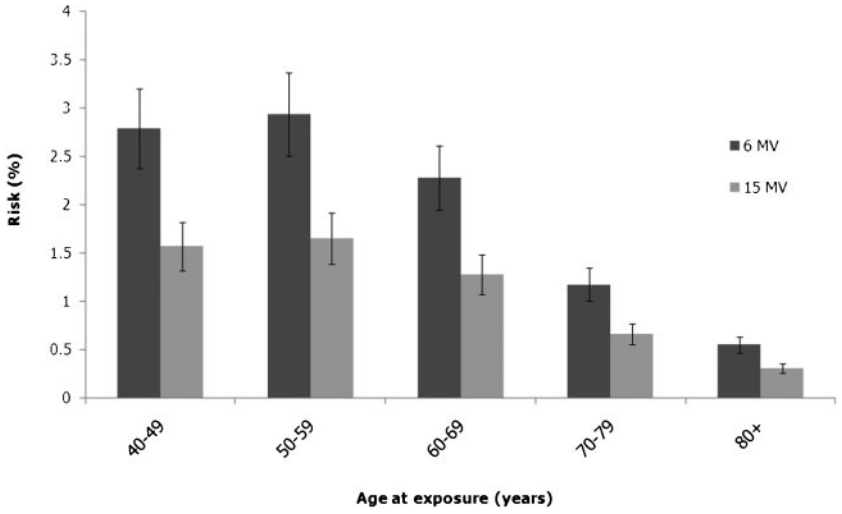

Figure 3. 40-year post exposure secondary cancer risk due to IMRT treatment for 6 and 15 MV. Error bars indicate the spread of risk estimates across the 5 patients.

through the verification of the IMRT plan, the same output conditions could be reconstructed within the phantom to give a similar radiation distribution. Organ risks were therefore specific to the Rando phantom and were satisfactory in making a comparison between the energies. It should also be noted that all solid organs except bone and lung were represented by the same tissue-equivalent material. There are also large uncertainties in determining the absolute risk of second cancer using current models, as discussed by Kry et al [50]. In this work, the risks calculated were not absolute but were compared relatively between the two energies.

In agreement with other authors [4, 45, 47, 51], our results indicate that the use of higher energies is dosimetrically comparable with 6 MV IMRT in prostate cancer patients, and is therefore a reasonable energy to be used. It was also observed that the time taken to produce a plan with 15 MV was less and used a lower number of MUs. There is currently (and there will be for years to come) a lack of epidemiological data on radiation-induced cancers due to IMRT, but our results indicate that 15 MV in prostate cancer patients may be associated with a lower out-of-field secondary cancer risk.

Conclusions

It has been shown that there is a small increased overall theoretical risk of developing a fatal cancer from 6 MV prostate IMRT compared with 15 MV prostate IMRT, taking into account all the organs. The theoretical risk of secondary induced malignancy in specific organs was also calculated, and it was found that for all out-of-field organs there is a moderate increased risk of developing a fatal cancer at 6 MV. The risk of developing fatal leukaemia was slightly raised at 6 MV compared with 15 MV, and risks of bladder or rectal cancer were similar at both energies. Conversely, there is a slightly raised rectal NTCP at 15 MV compared with 6 MV (3.6% compared with 3.0%, respectively). There also appears to be a reduction in TCP of around 0.3% at 15 MV compared with 6 MV ($p=0.049$); however, it is unlikely that this would have clinical significance. The weight of evidence suggests that photon energies above 10 MV should not be excluded in IMRT treatment. However, considering the lack of epidemiological data on radiation-induced cancer due to IMRT, it is recommended that the choice to treat at 15 MV is taken as a risk versus benefit decision, considering the age and life expectancy

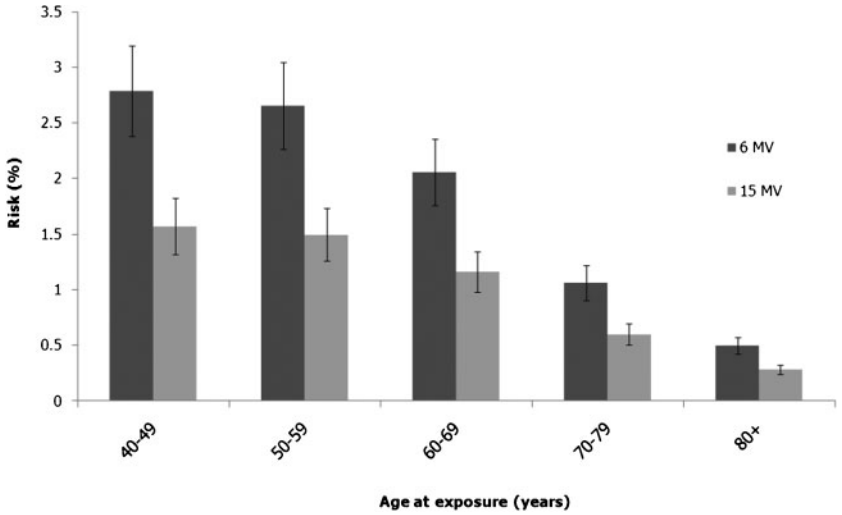

Figure 4. Lifetime risk of secondary induced cancer due to the IMRT treatment for 6 and 15 MV. Error bars indicate the spread of risk estimates across the 5 patients.

of the patient together with the relative risk of radiation-induced cancer and NTCPs.

Acknowledgments

The authors are grateful to the Regional Radiation Protection Service for providing use of their TLD facilities and the Rando phantom, and would like to thank Luke Hager and Dr Rick Tanner of the HPA for kindly providing and processing the neutron track etch detectors, and for their advice.

References

1. Intensity Modulated Radiation Therapy Collaborative Working Group. Intensity-modulated radiotherapy: current status and issues of interest. Int J Rad Oncol Biol Phys 2001;51:880–914.
2. Hall EJ. Intensity-modulated radiation therapy, protons, and the risk of secondary cancers. Int J Rad Oncol Biol Phys 2006;65:1–7.
3. d'Errico F. Dosimetric issues in radiation protection of radiotherapy patients. Rad Prot Dosim 2006;118:205–12.
4. Parzall A, Carol MP, Pickett B, Xia P, Roach M, Verhey LJ. The effect of beam energy and number of fields on photon-based IMRT for deep-seated targets. Int J Rad Oncol Biol Phys 2002;53:434–42.
5. Luxton G, Hancock SL, Boyer AL. Dosimetry and radiobiologic model comparison of IMRT and 3D conformal radiotherapy in treatment of carcinoma of the prostate. Int J Radiat Oncol Biol Phys 2004;59:267–84.
6. Ruben JD, Davis S, Evans C, Jones P, Gagliardi F, Haynes M, Hunter A. The effect of intensity-modulated radiotherapy on radiation-induced second malignancies. Int J Radiat Oncol Biol Phys 2008;70:1530–6.
7. Followill D, Geis P, Boyer A. Estimates of whole-body dose equivalent produced by beam intensity modulated conformal therapy. Int J Radiat Oncol Biol Phys 1997;38:667–72.
8. Hall EJ, Wuu C-S. Radiation-induced second cancers: the impact of 3D CRT and IMRT. Int J Radiat Oncol Biol Phys 2003;56:83–8.
9. Stathakis S, Li J, Ma CCM. Monte Carlo determination of radiation-induced cancer risks for prostate patients undergoing intensity-modulated radiation therapy. J Applied Clin Med Phys 2007;8:14–27.
10. Kry SF, Salehpour M, Followill DS, Stovall M, Kuban DA, White RA, Rosen II. The calculated risk of fatal secondary malignancies from intensity-modulated radiation therapy. Int J Rad Oncol Biol Phys 2005;62:1195–1203.
11. NCRP Report 116. Limitation of exposure to ionizing radiation. Bethesda, MD: National Council on Radiation Protection and Measurements, 1993.
12. Bostrom PJ, Soloway MS. Secondary cancer after radiotherapy for prostate cancer: should we be more aware of the risk? European Urology 2007;52:973–82.
13. Schneider U, Lomax A, Lombriser N. Comparative risk assessment of secondary cancer incidence after treatment of Hodgkin's disease with photon and proton radiation. Radiat Res 2000;154:382–8.
14. Miralbell R, Lomax A, Cella L, Schneider U. Potential reduction of the incidence of radiation-induced second cancers by using proton beams in the treatment of pediatric tumours. Int J Radiat Oncol Biol Phys 2002;54:824–29.
15. Upton AC. Radiobiological effects of low doses. Implications for radiological protection. Radiat Res 1977;71:51–74.
16. Daşu A, Toma-Daşu I, Olofsson J, Karlsson M. The use of risk estimation models for the induction of secondary cancers following radiotherapy. Acta Oncologica 2005;44:829–35.
17. UNSCEAR. Sources and effects of ionizing radiation 1993. Report to the General Assembly, with annexes. New York, NY: United Nations, 1993.
18. Khoo VS, Dearnaley DP. Question of dose, fractionation and technique: ingredients for testing hypofractionation in prostate cancer – the CHHiP trial. Clin Oncol 2008;20:12–14.
19. Sanchez-Nieto B, Nahum AE. BIOPLAN: software for the biological evaluation of radiotherapy treatment plan. Med Dosim 2000;25:71–6.
20. Webb S, Nahum AE. A model for calculating tumour control probability in radiotherapy including the effects of inhomogeneous distribution of dose and clonogenic cell density. Phys Med Biol 1993;38:653–66.
21. Sanchez-Nieto B, Nahum AE. The delta-TCP concept: a clinically useful measure of tumour control probability. Int J Radiat Oncol Biol Phys 1999;44:369–80.
22. Brenner DJ, Hall EJ. Fractionation and protraction for radiotherapy of prostate carcinoma. Int J Radiat Oncol Biol Phys 1999;43:1095–1101.
23. Zelefsky MJ, Chan H, Hunt M, Yamanda Y, Shippy AM, Amols H. Long-term outcome of high dose intensity modulated radiation therapy for patients with clinically localized prostate cancer. J Urol 2006;176:1415–19.
24. Levegrün S, Jackson A, Zelefsky MJ, Skwarchuck MW, Venkatraman ES, Schlegel W, et al. Fitting tumour control probability models to biopsy outcome after three-dimensional conformal radiation therapy for prostate cancer: pitfalls in deducing radiobiologic parameters for tumors from clinical data. Int J Rad Oncol Biol Phys 2001;51:1064–80.
25. Lyman JT. Complication probability as assessed from dose-volume histograms. Radiat Res 1985;8:S13–S19.
26. Niemierko A. A generalized concept of equivalent uniform dose (EUD). Med Phys 1999;26:1100.
27. Kutcher GJ, Burman C, Brewster L, et al. Histogram reduction method for calculating complication probabilities for three-dimensional treatment planning evaluations. Int J Radiat Oncol Biol Phys 1991;21:137–46.
28. Burman C, Kutcher GJ, Emami B, et al. Fitting of normal tissue tolerance data to an analytic function. Int J Radiat Oncol Biol Phys 1991;21:123–35.
29. Michalski JM, Gay H, Jackson A, Tucker SL, Deasy JO. Radiation dose-volume effects in radiation-induced rectal injury. Int J Radiat Oncol Biol Phys 2010;76:S123–9.
30. Viswanathan AN, Yorke ED, Marks LB, Eifel PJ, Shipley WU. Radiation dose-volume effects of the urinary bladder. Int J Radiat Oncol Biol Phys 2010;76:S116–22.
31. Fiorini CF, Valdagni R, Rancati T, Sanguineti G. Dose-volume effects of normal tissues in external radiotherapy: pelvis. Radiother Oncol 2009;93:153–67.
32. Emami B, Lyman J, Brown A, et al. Tolerance of normal tissue to therapeutic irradiation. Int J Rad Oncol Biol Phys 1991;21:109–22.
33. Alderson SW. Radio-therapy phantom. Patent number: 3 310 885. New York, 1967.
34. ICRP 103. The 2007 Recommendations of the International Commission on Radiological Protection. Oxford, UK: ICRP, 2007.
35. Ellis RE. The distribution of active bone marrow in the adult. Phys Med Biol 1961;5:255–8.
36. NCRP Report 151. Structural shielding design and evaluation for megavoltage X-ray and gamma-ray radiotherapy facilities. Bethesda, MD: National Council on Radiation Protection and Measurements, 2005.
37. Bartlett DT, Greenhalgh JR. Calculations of effective dose equivalent, ambient dose equivalent and individual dose equivalent for a set of reference neutron spectra and field geometries. Health Physics 1986;50:548–50.
38. Thomas DJ, Bardell AG, Macaulay EM. Characterisation of a gold foil-based Bonner sphere set and measurements of

neutron spectra at a medical accelerator. Nuc Instr and Meth A 2002;476:31–5.
39. Howell RM, Hertel NE, Wang Z, Hutchinson J, Fullerton GD. Calculation of effective dose from measurements of secondary neutron spectra and scattered photon dose from dynamic MLC IMRT for 6 MV, 15 MV, and 18 MV beam energies. Med Phys 2006;33:360–8.
40. Kry SF, Salehpour M, Followill DS, Stovall M, Kuban DA, White RA, Rosen II. Out-of-field photon and neutron dose equivalents from step-and-shoot intensity-modulated radiation therapy. Int J Rad Oncol Biol Phys 2005;62: 1204–16.
41. Muirhead CR, Cox R, Stather JW, MacGibbon BH, Edwards AA, Haylock RG. Estimates of late radiation risks to the UK population. Didcot, UK: NRPB, 1993;4.
42. Verellen D, Vanhavere F. Risk assessment of radiation-induced malignancies based on whole-body equivalent dose estimates for IMRT treatment in the head and neck region. Radioth Oncol 1999;53:199–203.
43. Ruben JD, Lancaster CM, Jones P, Smith RL. A comparison of out-of-field dose and its constituent components for intensity-modulated radiation therapy versus conformal radiation therapy: implications for carcinogenesis. Int J Rad Oncol Biol Phys In press.
44. Dorr W, Herrmann T. Second primary tumors after radiotherapy for malignancies. Strahlenther. Onkol 2002;178: 357–62.
45. Reft CS, Runkel-Muller R, Myrianthopoulos L. In vivo and photon measurements of secondary photon and neutron doses for prostate patients undergoing 18 MV IMRT. Med Phys 2006;33:3734–42.
46. Becker J, Brunckhorst E, Schmidt R. Investigation of the neutron contamination in IMRT deliveries with a paired magnesium and boron coated magnesium ionization chamber system. Radiother Oncol 2008;86:182–6.
47. Kry SF, Salehpour M, Titt U, White RA, Stovall M, Followill DS. Monte Carlo study shows no significant difference in second cancer risk between 6- and 18-MV intensity-modulated radiation therapy. Radiother Oncol 2009;91: 132–7.
48. Sachs RK, Brenner DJ. Solid tumour risks after high doses of ionizing radiation. PNAS 2005;102:13 040–5.
49. Shuryak I, Sachs RK, Hlatky L, Little MP, Hahnfeldt P, Brenner DJ. Radiation-induced leukemia at doses relevant to radiation therapy: modelling mechanisms and estimating risk. J Natl Cancer Inst 2006;98:1794–1806.
50. Kry SF, Followill D, White RA, Stovall M, Kuban DA, Salehpour M. Uncertainty of calculated risk estimates for secondary malignancies after radiotherapy. Int J Radiat Oncol Biol Phys 2007;68:1265–71.
51. Aoyama H, Westerly DC, Mackie TM, Olivera GH, Bentzen SM, Patel RR, et al. Integral radiation dose to normal structures with conformal external beam radiation. Int J Rad Oncol Biol Phys 2006;64:962–67.